World Scientific
www.worldscientific.com

STRUCTURE OF IONS AND WATER AROUND A POLYELECTROLYTE IN A POLARIZABLE NANOPORE

LEI GUO and ERIK LUIJTEN*

Department of Materials Science and Engineering
University of Illinois at Urbana-Champaign
1304 W Green Street Urbana, IL 61801, USA
*luijten@northwestern.edu

We study the distribution of ions and water within a pore in a polarizable membrane, in the presence of a stiff polyelectrolyte threaded through the pore. In this system, which represents a typical situation during the translocation of DNA, the distribution of both the ions and the water molecules is affected by the induced charges on the surface of the polarizable nanopore. Specifically, the concentration of counterions is enhanced near the surface of the pore, due to the attractive interaction with the induced charges. Conversely, the water within the pore is depleted, as a result of the disruption of hydrogen bonds by the induced charges.

1. Introduction

Translocation of genetic material (i.e. DNA and RNA) through nanopores in cell membranes is a ubiquitous phenomenon in nature.[1] Recently, the translocation of DNA through a nanopore, driven by an electric field, has been achieved in experiments.[2–4] Fundamentally, the translocation experiment provides a model system for the study of the complicated behavior of a polyelectrolyte and its associated ions under nano-confinement. Technically, it may provide the starting point for the construction of an efficient and economical device for sequencing DNA. The idea behind DNA-sequencing using a nanopore is simple: the ionic current induced by the electric field will be reduced as DNA passes through the pore, due to the partial blockage of the pore by the DNA. Since the building blocks of DNA, i.e. the nucleotides, have distinct structures, the blockage of the ionic current will depend on the type of nucleotide that resides within the pore. Therefore, in principle DNA can be sequenced by recording the variation of the measured ionic current. The feasibility of this idea has been demonstrated in several pioneering works.[2,3] However,

---

*Present address: Department of Materials Science and Engineering, Department of Engineering Sciences and Applied Mathematics, Northwestern University, Evanston, IL 60208, USA.

while seemingly straightforward, these experiments can yield complicated results depending on the experimental conditions. As shown in Refs. 5 and 6, at low salt concentrations the ionic current is *enhanced* when DNA is translocating through the nanopore, contrary to the above-described behavior at high salt concentrations.[2,3] Understanding the dependence of the ionic current on salt concentration requires the study of the behavior of DNA and its counterions under confinement. Computer simulations are particularly suitable for studying the behavior *within* the pore, as this is not easily accessible in experiments. However, the modeling of the nanopore can also bring challenges, e.g. if the pore is embedded in a polarizable membrane. In that case, charges will be induced on the surface of the nanopore during the passage of DNA and its associated ions. Until now, the effect of these induced charges on the translocation process is unclear. It is our objective in this paper to study the effect of membrane polarizability on charged molecules under confinement. Our molecular dynamics simulations thus may form a first step toward understanding some phenomena observed in DNA translocation experiments.

To approach the problem systematically, in this paper we concentrate on the *equilibrium* structure of ions and water within a nanopore in the presence of a *stiff* immobile polyelectrolyte. The choice of a stiff chain has the advantage of decoupling the chain conformation from its interaction with the ions. Indeed, the dimensions chosen in the present work correspond to single-stranded DNA (the most widely used molecule in translocation experiments), which is a flexible molecule. However, it is not unrealistic to approximate a short threaded segment as a stiff rod. As an additional justification, we note that various biological polyelectrolytes are indeed stiff molecules on the scale of the nanopore, including double-stranded DNA (ds-DNA), actin filaments, and microtubules. Especially, recent experiments have begun to study the translocation of ds-DNA through a nanopore.[5] As a further simplification, we fix the stiff polyelectrolyte in the center of the pore, and focus on the distribution of ions and water as a function of membrane polarizability. This polarizability is accounted for by means of a grid-based self-consistent numerical calculation of the induced charges during the molecular dynamics simulations.[7–9] The induced charges need to be calculated in each simulation step, and each particle in the system will experience additional electrostatic forces from these charges.

2. Simulation Model and Techniques

The molecular dynamics simulation package LAMMPS[10] is employed in this work. Figure 1 shows the simulation cell. The rectangular system is periodic in all three spatial directions and has fixed dimensions of $L_{x,y} = 60$ Å in both the x and the y direction (perpendicular to the pore), whereas the z-dimension (parallel to the pore) is controlled by the external pressure $P = 1.013$ bar of the applied *NPT* ensemble; it has an average value $\langle L_z \rangle = 86.2 \pm 0.3$ Å. The pressure is controlled via a Nosé–Hoover barostat and the temperature, which is fixed at 300 K, by a Nosé–Hoover thermostat. The membrane has a thickness of 42 Å with a cylindrical pore of radius
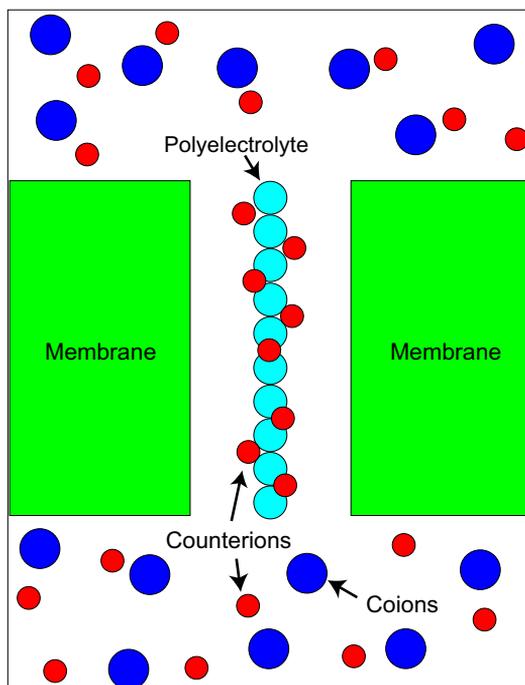
Fig. 1.   Schematic setup of the simulation system (two-dimensional cross-section): The stiff polyelectrolyte is fixed in the center of the pore, which is embedded in the membrane; dark (larger) and lighter (smaller) spheres represent coions and counterions, respectively; the water molecules (represented by the SPC/E model) are not shown.

6.5 Å (owing to the particle–membrane interactions, the *effective* radius of the pore is approximately 4.5 Å). A *stiff* linear polyelectrolyte, consisting of 10 spherical monomers of radius 2.1 Å, is fixed in the center of this pore. The linear charge density of the polyelectrolyte is $-1e/4.2$ Å (i.e. one elementary charge on each of the monomers), comparable to that of the single-stranded DNA. The system contains 188 monovalent salt ions, corresponding to 94 KCl molecules (equivalent to the 1 M salt concentration employed in the experiments[2,3]), as well as 10 additional K^+ ions that act as counterions to the polyelectrolyte. Because of the small dimensions of the nanopore, it is highly ambiguous to use an implicit water model within the pore, so that we employ an explicit water model in this study. Each water molecule is modeled via the SPC/E model,[11] consisting of three point charges, representing one oxygen and two hydrogen atoms. The system contains a total of 4950 SPC/E water molecules, which constitutes a large computational hurdle. To accelerate the simulations, we fix the H—O bond lengths and the H—O—H angle of each water molecule using the SHAKE algorithm,[12] which makes it possible to increase the simulation time step to 2 fs. The electrostatic interactions are computed using the particle–particle particle–mesh Ewald method, which scales as $N \log N$ (N is

the total number of point charges in the system) and is considerably faster than the conventional Ewald method (which requires a computational effort $\mathcal{O}(N^{3/2})$) for sufficiently large values of N.[13] The particle–particle and particle–wall interactions are modeled by means of Lennard-Jones potentials, where the wall is modeled according to Appendix A of Ref. 9 and the Lennard-Jones parameters correspond to Table 1 of Ref. 14.

The membrane itself is modeled as a dielectric continuum with a dielectric constant ε_m. In order to incorporate the effect of membrane polarizability, we assume that it has a sharp dielectric boundary with the solution. This assumption implies that the induced charges are located only on the surface of the membrane and the pore, which in turn greatly reduces the effort required to calculate the polarization charges. These charges are discretized by overlaying a grid on the surface of the membrane and the nanopore. In our system, the grid is composed of 2150 points, 1722 of which form a square lattice on the inner surface of the pore, whereas 428 more points lie on the outer surface of the membrane in concentric rings around the pore openings (the largest of these rings has a radius of 10 Å). The charge on each grid point, which corresponds to a surface area of approximately 1.0 Å^2, is obtained via a self-consistent method that is equivalent to solving the Poisson equation.[7] Since the full self-consistent calculation is time-consuming, it is performed only after every 100 simulation steps. At the intermediate time steps between each full calculation, an approximation is employed.[9] The calculated induced charges exert additional electrostatic forces on every particle in the system and thus influence the evolution of the system. For details of the calculation of the induced charges see Ref. 7.

The total simulation time amounts to 12 ns (6×10^6 timesteps) for the nonpolarizable ($\varepsilon_m = 1$) case, and 2 ns (1×10^6 timesteps) for the computationally much more demanding polarizable ($\varepsilon_m > 1$) case.

3. Results and Discussion

We characterize the distribution of ions and water molecules inside the nanopore by means of the radial distribution function $n(r)$, the number of particles within the pore at a distance r from the central axis. To study the effect of membrane polarizability, the simulations are carried out at three different values for the membrane dielectric constant: $\varepsilon_m = 1.0$, 2.0, and 20.0. We find that the Cl$^-$ coions, which are strongly repelled by the anionic polyelectrolyte, do not enter the pore. The distribution $n_{\mathrm{K}}(r)$ of the K$^+$ counterions is shown in Fig. 2. The depletion of ions near the center of the pore ($r \lesssim 2$ Å) simply reflects the excluded volume of the polyelectrolyte. This is followed by a peak at $r = 2.4 \pm 0.1$ Å, arising from the counterions that are condensing on the polyelectrolyte. However, upon increase of ε_m (i.e. with increasing membrane polarizability) the counterion distribution widens. This is a seemingly counterintuitive result, since our calculation also shows that the average number of counterions within the pore is not sufficient to neutralize the
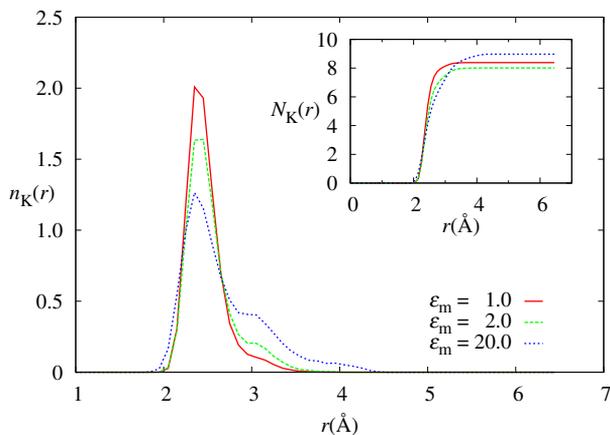
Fig. 2.   Radial distribution of K^+ counterions within the $R = 6.5$ Å pore. The curves from top to bottom represent the system with membrane dielectric constant $\varepsilon_m = 1.0$, 2.0, and 20.0, respectively. All curves approach zero around $r = 4.5$ Å, which is the *effective* radius of the pore, as determined by the ion–membrane interactions. The inset shows the corresponding *cumulative* counterion distributions. In all cases, the number of counterions is less than needed to fully neutralize the polyelectrolyte.

polyelectrolyte, see inset of Fig. 2. Accordingly, the net charge within the pore is negative and one thus expects a positive induced charge on the nanopore surface (since the *net* induced charge on the membrane must be zero, this would then in turn have to be compensated by negative induced charges at the outer surface of the membrane), leading to a repulsive force on the counterions that increases with increasing membrane polarizability. However, this simple argument proves to be incorrect, owing to local fluctuations of the induced charges. We observe that, if a counterion approaches the nanopore surface, it locally induces a negative charge, which in turn *attracts* the ion. Consistent with this observation, we find that the fluctuations in the induced charge increase with increasing ε_m, see Fig. 3.

Interestingly, also the structure of water inside the pore is strongly affected by the membrane polarizability. Figure 4 shows the radial distribution $n_O(r)$ of oxygen atoms. With increasing ε_m the area below the curve, i.e. the total number of water molecules within the pore, decreases. Interestingly, such depletion was *not* observed in a study of a polarizable nanopore (also with SPC/E water) in the absence of a polyelectrolyte and counterions.[9] Indeed, in that study, the membrane polarizability was found to *enhance* the permeation of water through a narrow pore ($R = 5.5$ Å), which was explained from a lowering of the free-energy barrier for a water molecule to translocate through an otherwise hydrophobic pore.[9] In the case studied here, the water molecules form a layered structure around the polyelectrolyte. The presence of induced charges disrupts this tightly bound structure and thus lowers the packing fraction of water inside the pore. The above-mentioned charge fluctuations induced by the mobile counterions further enhance this effect. To support this
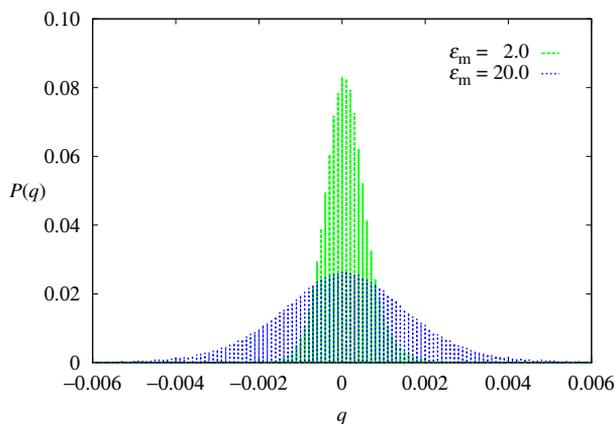
Fig. 3.   Normalized induced charge distribution on the surface of the $R = 6.5$ Å pore with $\varepsilon_m = 2.0$ and 20.0, respectively. The charge is expressed in units of elementary charge per grid point. A larger polarizability leads to stronger charge fluctuations, because the system responds more strongly to the behavior of mobile charge carriers (counterions).
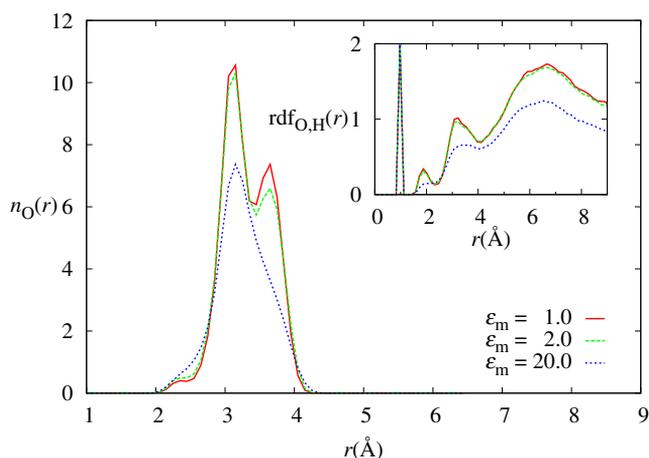
Fig. 4.   Water distribution (represented by the position of its oxygen atom) along the radial distance r from the center of the $R = 6.5$ Å pore, for $\varepsilon_m = 1.0$, 2.0, and 20.0, respectively. The area under the curves decreases with increasing membrane dielectric constant, implying a decreasing water content within the pore. The inset shows the corresponding oxygen–hydrogen pair correlation functions, which support the hypothesis that the network of hydrogen bonds is disrupted as the polarizability increases.

explanation, we characterize the water structure by means of the oxygen–hydrogen pair correlation function, see the inset of Fig. 4. The short-distance peak in this correlation function simply reflects the internal oxygen–hydrogen bonds of a water molecule (bond length 1 Å). The second peak around $r = 2.0$ Å characterizes the hydrogen bonds formed between water molecules inside the pore. The magnitude of this second peak indeed decreases as ε_m increases, confirming the disruption of

hydrogen bonds as the membrane polarizability increases. We note that the decrease in the second peak is not merely due to the depletion of water from the pore.

4. Conclusion

We have considered a stiff, highly charged polyelectrolyte within a nanopore in a polarizable membrane. In order to understand the effect of an external electric field, such as employed in DNA translocation experiments, on the polyelectrolyte, we have determined the distribution of ions and water molecules within the nanopore by means of molecular dynamics simulations. In particular, we have focused on the effect of membrane polarizability, employing a recently developed calculation method for the induced charges on the inner surface of the pore. We find two prominent effects of polarizability. First, increasing the membrane dielectric constant leads to an increased tendency of the counterions to reside near the pore surface, resulting in an inhomogeneous distribution of the polarization charges. Secondly, water is depleted from the pore as the polarizability increases, which we ascribe to the disruption by the induced charges of a tightly bound arrangement of water molecules around the polyelectrolyte. Even though our simulations employ a coarse-grained model for the polyelectrolyte and the membrane surface, they offer interesting insights in the effects of polarization charges on the structural arrangement of charge carriers within a nanopore.

In the near future, we will extend this study to the case of a flexible polyelectrolyte and to situations with an external electric field, making it possible to forge direct connections with experimental observations.

References

1. B. Alberts, A. Johnson, J. Lewis, M. Raff, K. Roberts and P. Walter, *Molecular Biology of the Cell*, 4th edn. (Garland Science, New York, 2002).
2. J. J. Kasianowicz, E. Brandin, D. Branton and D. W. Deamer, *Proc. Natl. Acad. Sci. USA* **93**, 13770 (1996).
3. A. Meller, L. Nivon and D. Branton, *Phys. Rev. Lett.* **86**, 3435 (2001).
4. A. J. Storm, C. Storm, J. Chen, H. Zandbergen, J.-F. Joanny and C. Dekker, *Nano Letters* **5**, 1193 (2005).
5. H. Chang, F. Kosari, G. Andreadakis, M. A. Alam, G. Vasmatzis and R. Bashir, *Nano Letters* **4**, 1551 (2004).
6. R. Fan, R. Karnik, M. Yue, D. Li, A. Majumdar and P. Yang, *Nano Letters* **5**, 1633 (2005).

7. R. Allen, J.-P. Hansen and S. Melchionna, *Phys. Chem. Chem. Phys.* **3**, 4177 (2001).

8. R. Allen, J.-P. Hansen and S. Melchionna, *Phys. Rev. Lett.* **89**, 175502 (2002).

9. R. Allen, J.-P. Hansen and S. Melchionna, *J. Chem. Phys.* **119**, 3905 (2003).

10. S. J. Plimpton, *J. Comp. Phys.* **117**, 1 (1995).

11. H. J. C. Berendsen, J. R. Grigera and T. P. Straatsma, *J. Phys. Chem.* **91**, 6269 (1987).

12. J.-P. Ryckaert, G. Ciccotti and H. J. C. Berendsen, *J. Comp. Phys.* **23**, 327 (1977).

13. D. Frenkel and B. Smit, *Understanding Molecular Simulation*, 2nd edn. (Academic, San Diego, 2002).

14. J. Dzubiella and J.-P. Hansen, *J. Chem. Phys.* **122**, 234706 (2005).